

Paper No.
16443



Methodology for Corrosion Inhibitor Characterization Applied to Phosphate Ester and Tetrahydropyrimidinium Model Compounds

Shuai Ren, Yi He, Zineb Belarbi, Xi Wang, David Young, Marc Singer

Institute for Corrosion and Multiphase Technology

Department of Chemical and Biomolecular Engineering

Ohio University

342 West State Street

Athens, OH 45701, USA

Maalek Mohamed-Saïd
TOTAL E&P

CSTJF, Avenue Larribau
Pau 64018, FRANCE

Sheyla Camperos
TOTAL RC

TRTG, TOTAL Research & Technology
Gonfreville
BP 27, Harfleur 76700, FRANCE

ABSTRACT

Organic corrosion inhibitors (CIs) are widely employed in the oil and gas industry to protect carbon steel pipelines against internal corrosion. Inhibitor selection by corrosion engineers frequently relies on long testing procedures and protocols, which requires significant time and expenditure. This study aims at providing a simpler and more reliable methodology for inhibitor characterization, which can contribute to inhibitor selection in the oil and gas industry. Two model compounds, tetradecyl phosphate ester (TPE) and tetradecyl tetrahydropyrimidinium (TTHP), were chosen for this methodology development in an aqueous environment of 5 wt.% NaCl (pH = 4.5) at 25°C. Linear polarization resistance (LPR) measurements were conducted to determine the corrosion rate (CR) over a wide range of CI concentrations, from which surface saturation concentration and surface coverage (θ) values were extracted. Kinetic parameters for adsorption (k_A , k_D , and K_{AD}) were obtained by means of Langmuir adsorption isotherm and non-linear regression analysis. Potentiodynamic polarizations were executed to analyze the inhibition behaviors. It is concluded that both TPE and TTHP could retard anodic and cathodic reactions with no change in limiting current.

Keywords: corrosion inhibitors, phosphate ester, tetrahydropyrimidinium, surface saturation concentration, adsorption kinetics

INTRODUCTION

Corrosion inhibitors (CIs) are widely used in the oil and gas industry to protect carbon steel tubulars against internal corrosion. CIs can be injected continuously into a corrosive environment at very low concentrations to decrease the corrosion rate of the exposed metallic material and maintain effective corrosion protection¹. CO₂ corrosion inhibitors typically consist of amphiphilic, surface-active molecules with alkyl tails typically in the range of C12 to C18². Such molecules have a strong tendency to adsorb onto the steel surface and form self-assembled structures^{3,4}.

However, the performance of these surfactant-type CIs is influenced by operating conditions, such as temperature, pressure, pH, and flow. If a corrosion inhibitor is added without considering these factors, its efficiency could be decreased and sometimes lost, which may result in unpredictable behavior and corrosion-related failures⁵⁻⁷. Generally, operators in the field find it very hard to predict CIs performance in advance, if there is any change in the operating condition. Consequently, an effective corrosion prediction tool would be indeed of great value. The long term objective of this work is to develop such an inhibition prediction tool, using, as a starting point, the inhibition model proposed by Dominguez Olivo^{8,9}. For now, the goal of this study is to develop a methodology for CI characterization valid in a wide range of conditions, which can be used for CI selection and dosing strategy. So far, the practice of corrosion inhibitor selection for corrosion engineers in the oil and gas industry usually relies on long testing procedures and protocols⁶. This practice requires excess time, which could be shortened with the development of methodology for CI characterization.

The research described herein focuses on developing a comprehensive and relevant methodology for CI characterization and inhibition evaluation. Two CI model compounds, tetradecyl phosphate ester (TPE) and tetradecyl tetrahydropyrimidinium (TTHP), were employed for this methodology development, which was performed in an aqueous environment of 5 wt.% NaCl (pH = 4.5) at 25°C. Surface saturation concentrations determined by evolution of linear polarization resistance (LPR) are reported with different concentrations of corrosion inhibitors (CIs), from which surface coverage (θ) values have been calculated. The kinetic parameters of adsorption (k_A , k_D , and K_{AD}) were obtained by means of a Langmuir adsorption isotherm and non-linear regression analysis. Finally, the inhibition behaviors were evaluated by means of potentiodynamic polarization curves.

EXPERIMENTAL SETUP AND METHODOLOGY

Materials and Chemicals

Steel specimens used for electrochemical measurements were machined from UNS G10180 carbon steel (C1018) with a ferritic-pearlitic microstructure, shown in Figure 1. The chemical composition of this carbon steel is provided in Table 1.

Table 1
Composition (wt.%) of C1018 mild steel

Element	C	Al	Cu	Mn	Cr	Mo	Ni	S	Si	Fe
Composition	0.15	0.096	0.032	0.78	0.017	0.019	0.032	0.017	0.21	balance

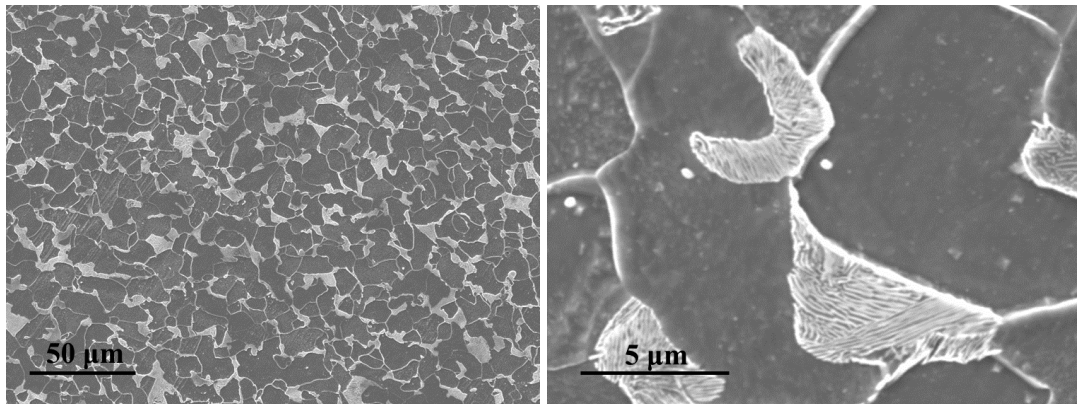


Figure 1: SEM images of ferritic-pearlitic microstructure of C1018.

Two CI model compounds employed in this work, *i.e.*, tetradecyl phosphate ester (TPE) and tetradecyl tetrahydropyrimidinium (TTHP), were synthesized in-house¹⁰. The composition of TPE consists of 73.5% monoester and 26.5% diester and the purity of TTHP is almost 100%. Their molecular structures are shown in Figure 2.

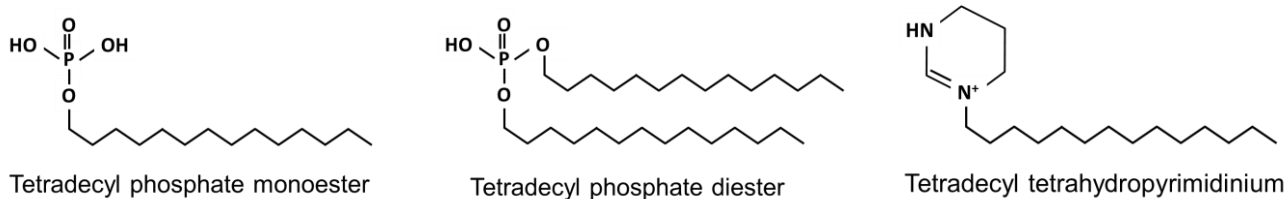


Figure 2: Molecular structures of CI model compounds (monoester and diester present as mixture)

Apparatus and Electrochemical Techniques

The electrochemical measurements were carried out using a three-electrode glass cell (Figure 3) with a platinum grid as a counter electrode, saturated KCl Ag/AgCl reference electrode, and a C1018 rotating cylinder electrode (RCE) with an outer diameter of 12 mm and a height of 14 mm as a working electrode. All potentials reported in this paper are in reference to a saturated KCl Ag/AgCl electrode. The reference electrode was connected to the corrosion cell *via* a KCl salt bridge and a Luggin capillary.

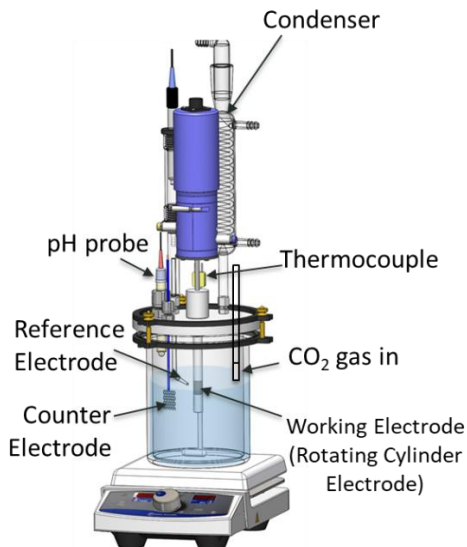


Figure 3: Schematic of the setup for electrochemical experiments[†]

Corrosion rate was assessed by linear polarization resistance (LPR) measurements, with a scan range from -5 mV to +5 mV vs. OCP, a scan rate of 0.125 mV/s and a B value of 26 mV. The B value for these experiments is taken from previous research conducted on mild steel in a CO₂ environment and was used in the analysis of all the experiments reported here¹¹. EIS data were acquired from 10 kHz to 0.02 Hz with 10 points per decade and a perturbation amplitude of 10 mV (rms). Cathodic potentiodynamic polarization sweeps were conducted at the end of each experiment when the corrosion rates were stable, by starting from the OCP down to -0.6 V vs. OCP at a scan rate of 0.125 mV/s. The anodic potentiodynamic sweeps were taken subsequently when the OCP returned to the original value before the cathodic sweep; they were taken from the OCP up to +0.2 V vs. OCP. The ohmic drop was compensated for in all the presented curves. All electrochemical tests were carried out via a potentiostat (Gamry Interface 1010[‡]).

Procedure and Test Matrix

Prior to each experiment, the RCE was sequentially polished with 180, 400 and 600 grit silicon carbide abrasive papers, cleaned with isopropanol in an ultrasonic bath after polishing, and air-dried before insertion into the cell. The corrosion tests were performed in 5 wt.% NaCl at 25°C and 1 bar total pressure. The solution was deoxygenated for 2 hours by sparging with CO₂ prior to the introduction of the working electrode. The CO₂ saturated solution was maintained at pH 4.5 by injecting NaHCO₃ and HCl solutions. Sparging with CO₂ was maintained throughout the test to prevent air ingress and maintain the saturation of the test electrolyte with CO₂. The rotation speed of the working RCE was set at 1000 rpm before starting the electrochemical measurements. Cl⁻s were dissolved in isopropyl alcohol first and then this mixture was deoxygenated with N₂ and injected into solution directly using a long syringe needle.

[†] Image courtesy of Cody Shafer, ICMT, Ohio University.

[‡] Trade name

Before the injection of Cls, there was 20 minutes of pre-corrosion, in which LPR, OCP and EIS measurements were taken to ensure that there was no contamination from previous experiments and the surface conditions of the steel specimens were consistent among all sets of tests. After the injection of Cls, LPR and EIS data were taken every 30 minutes until the corrosion rate became stable (± 0.01 mm/year). At the end of each test, potentiodynamic polarizations were conducted. A schematic of the experimental procedure is shown in Figure 4. All tests were repeated at least once to ensure their repeatability. As for test environment, 5 wt.% NaCl was used as the electrolyte for all tests to simulate the exploration and production environment in oil and gas industry, where the produced water often contains high salt concentration¹². The full experimental matrix for electrochemical experiments is shown in Table 2.

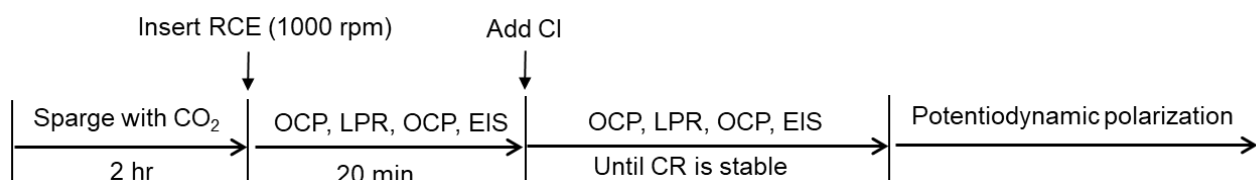


Figure 4: General experimental procedure for electrochemical experiments

Table 2
Experimental matrix for electrochemical experiments

Description	Parameters
Working solution	5 wt.% NaCl
Material	UNS G10180
Total pressure	1 bar
CO ₂ partial pressure	0.96 bar
Temperature	25 °C
pH	4.5 ± 0.1
Cl model compound	TPE and TTHP

EXPERIMENTAL RESULTS AND DISCUSSION

Determination of Surface Saturation Concentration

As described by Hackerman, *et al.*¹³, the surface saturation concentration is the critical bulk Cl concentration for which the metal surface is assumed to be saturated with the adsorbed inhibitor molecules, resulting in minimal corrosion rate and maximal inhibition efficiency. It can be determined by comparing the stable corrosion rates of metal specimens exposed to different Cl concentrations.

Corrosion Rate Analysis

Results of corrosion rate evolution with time in various TPE and TTHP concentrations, at the test condition, are shown in Figure 5 and Figure 6, respectively. From the results, the corrosion rate stabilized at around 2 mm/year in the blank test without inhibitor. With addition of 3 mL isopropanol but no Cl, the corrosion rate was very close to the corrosion rate in the uninhibited environment, which indicated that the injection of isopropanol as solvent for the Cls had no influence on corrosion rate. When the Cls were added into the solution, the corrosion rate initially decreased and then stabilized with time for each tested concentration.

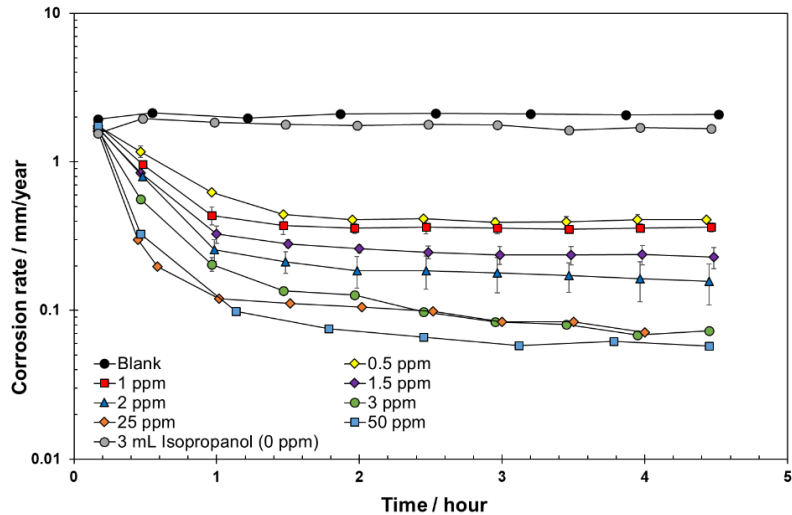


Figure 5: Corrosion rate vs. time of C1018 in 5 wt.% NaCl (pH = 4.5) with different TPE concentrations at 25°C.

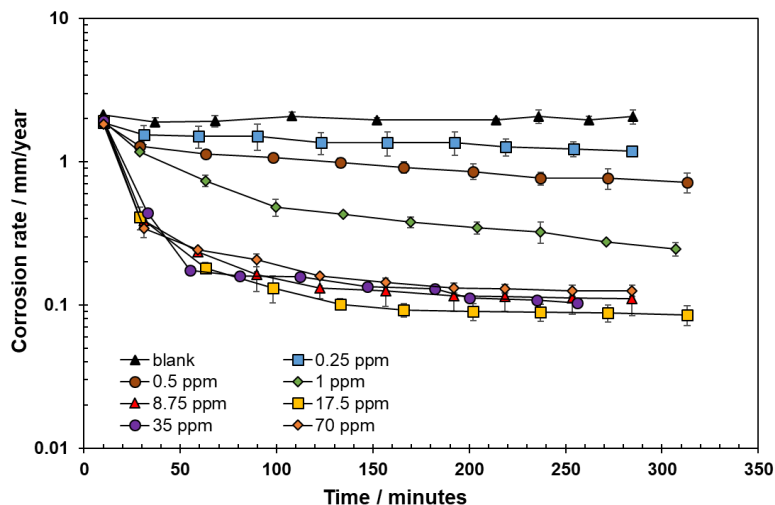


Figure 6: Corrosion rate vs. time of C1018 in 5 wt.% NaCl (pH = 4.5) with different TTHP concentrations at 25°C.

According to the results shown in Figure 5, the stable corrosion rate decreased with increasing TPE concentration when the concentration was no more than 2 ppm_w. This implies that the inhibition effect on the corrosion of C1018 increases with the increasing of TPE concentration. However, when the Cl concentration surpassed 3 ppm_w, the corrosion rate of C1018 did not decrease further and stabilized at around 0.08 mm/year. This indicates that the surface saturation for TPE was achieved to maximize the inhibition effect. Therefore, the critical concentration for TPE to achieve surface saturation in 5 wt.% NaCl was between 2 to 3 ppm_w. Similarly, the equivalent experimental results obtained with TTHP display the same trend and the surface saturation concentration in the test electrolyte was determined to be between 1 and 8.75 ppm_w.

It is noteworthy that the initial corrosion rates measured shortly before the injection of CIs were quite close to it measured in the blank test, which means the solution conditions before injection of CIs were

nearly identical to the blank solution. Therefore, there was no inhibitor contamination by previous experiments.

Open Circuit Potential (OCP)

The trends of open circuit potential with time, at different TPE and TTDP concentrations, are displayed in Figure 7 and Figure 8, respectively. The OCP fluctuations can provide qualitative information about the state of the electrode surface and, in this case, can provide indication of Cl⁻ adsorption. Without Cl⁻s, the OCP stabilized around -0.73 V to -0.68 V vs. saturated KCl Ag/AgCl. After adding Cl⁻s, the OCP increased sharply to about -0.66 V vs. saturated KCl Ag/AgCl and then stabilized with time. However, neither corrosion rate or OCP could indicate whether the anodic or cathodic reaction was retarded. Potentiodynamic polarization measurements serve to elucidate which electrochemical processes are responsible for the decreases in observed corrosion rates.

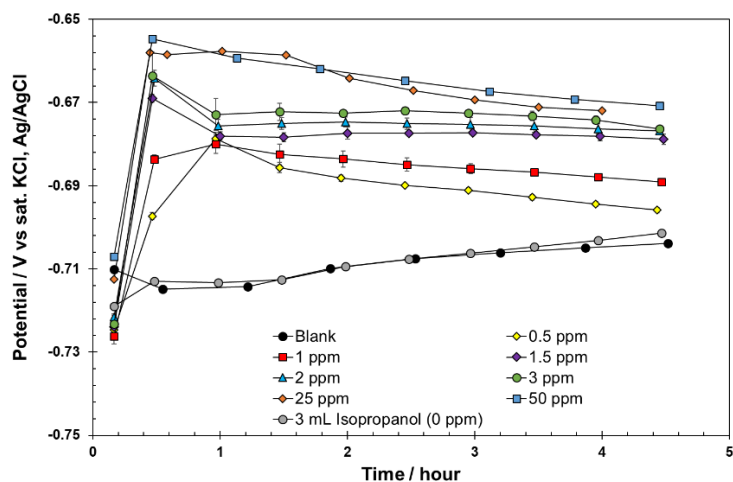


Figure 7: Open circuit potentials of C1018 in 5 wt.% NaCl (pH = 4.5) with different TPE concentrations at 25°C.

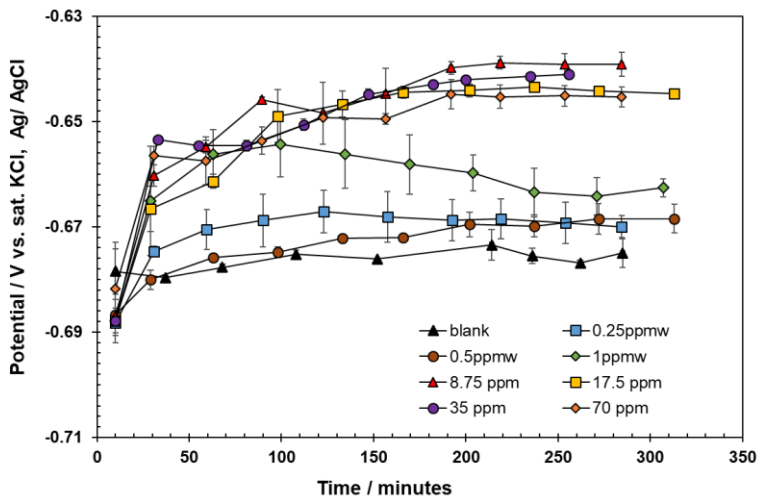


Figure 8: Open circuit potentials of C1018 in 5 wt.% NaCl (pH = 4.5) with different TTHP concentrations at 25°C.

Potentiodynamic Polarization

Potentiodynamic polarization curves of C1018 in 5 wt.% NaCl (pH = 4.5) with different TPE and TTHP concentrations at 25°C are shown in Figure 9 and Figure 10, respectively. Comparing the tests containing TPE or TTHP with the blank tests, both anodic and cathodic polarization curves were retarded. However, limiting currents remained unaffected. The inhibition behavior is similar to what was previously observed for a X65 steel inhibited with quaternary ammonium model compounds^{8,9}. Therefore, the model developed by Domínguez Olivo, *et al.*^{8,9}, seems applicable to the TPE and TTHP model compounds. Besides, for both TPE and TTHP, the fact that polarization curves with higher concentrations than their surface saturation concentrations almost overlapped with each other is consistent with the results of corrosion rate and OCP.

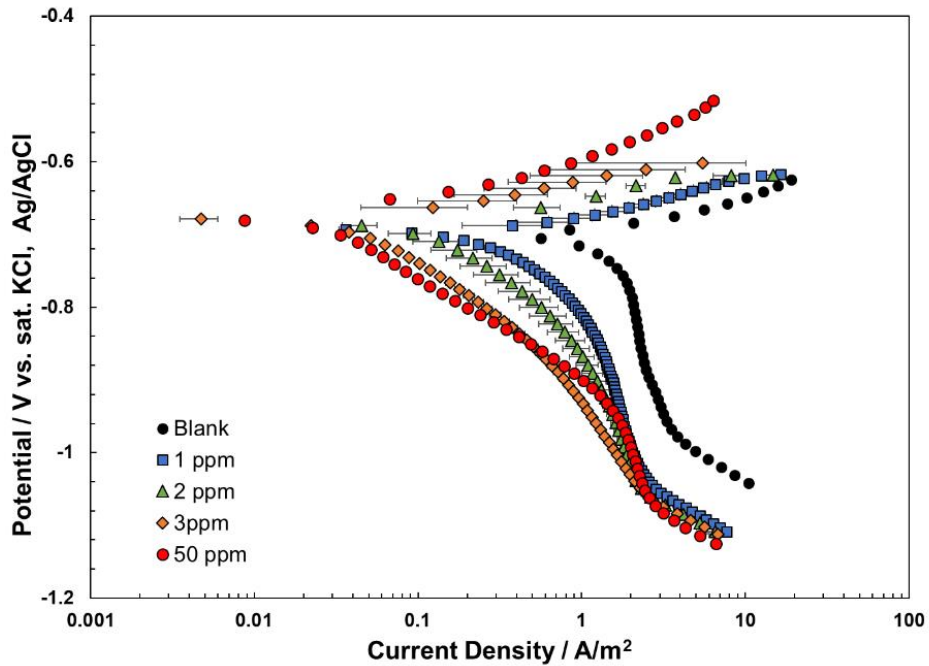


Figure 9: Potentiodynamic polarization curves of C1018 in 5 wt.% NaCl (pH = 4.5) with different TPE concentrations at 25°C.

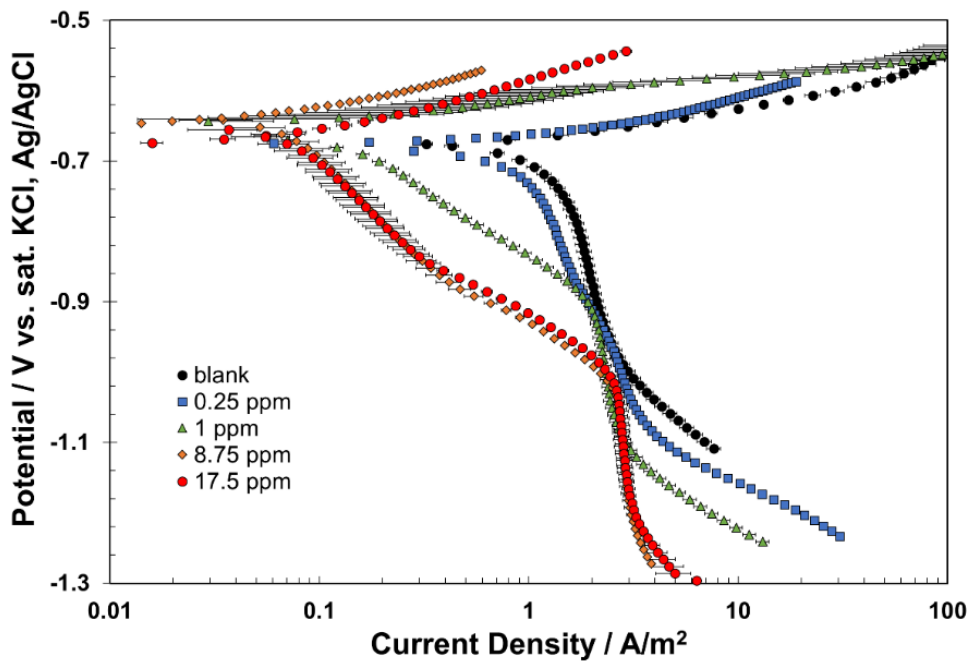


Figure 10: Potentiodynamic polarization curves of C1018 in 5 wt.% NaCl (pH = 4.5) with different TTHP concentrations at 25°C.

Determination of Kinetic Parameters of Adsorption

Surface Coverage Fraction (θ)

According to the work of Hackerman, *et al.*, ¹³ the inhibitor molecules coverage fraction on a metal surface can be calculated by Equation (1):

$$\theta = \frac{(i_{corr})_{\theta=0} - (i_{corr})_{\theta}}{(i_{corr})_{\theta=0} - (i_{corr})_{\theta_{max}}} \quad (1)$$

where $(i_{corr})_{\theta=0}$ is the corrosion rate without Cl, $(i_{corr})_{\theta}$ is the corrosion rate with Cl, and $(i_{corr})_{\theta_{max}}$ is the steady-state corrosion rate with Cl at the surface saturation concentration with maximum surface coverage.

The corrosion rates shown in Figure 5 and Figure 6 were then converted into the coverage fraction for C1018 in 5 wt.% NaCl with different TPE and TTHP concentrations as plotted in Figure 11 and Figure 12, respectively. The coverage fraction at steady state, *i.e.*, equilibrium coverage fraction (θ_{eq}), can be obtained by plugging steady state corrosion rate into Equation (1). The equilibrium coverage fractions for different TPE and TTHP concentrations are listed in Table 3 and Table 4, respectively. When the concentration is greater than surface saturation concentration, the equilibrium coverage is considered to have reached its maximum value, *i.e.*, full coverage. In the next section, these values of coverage fraction are employed in determination of kinetic parameters of Cl molecules adsorption.

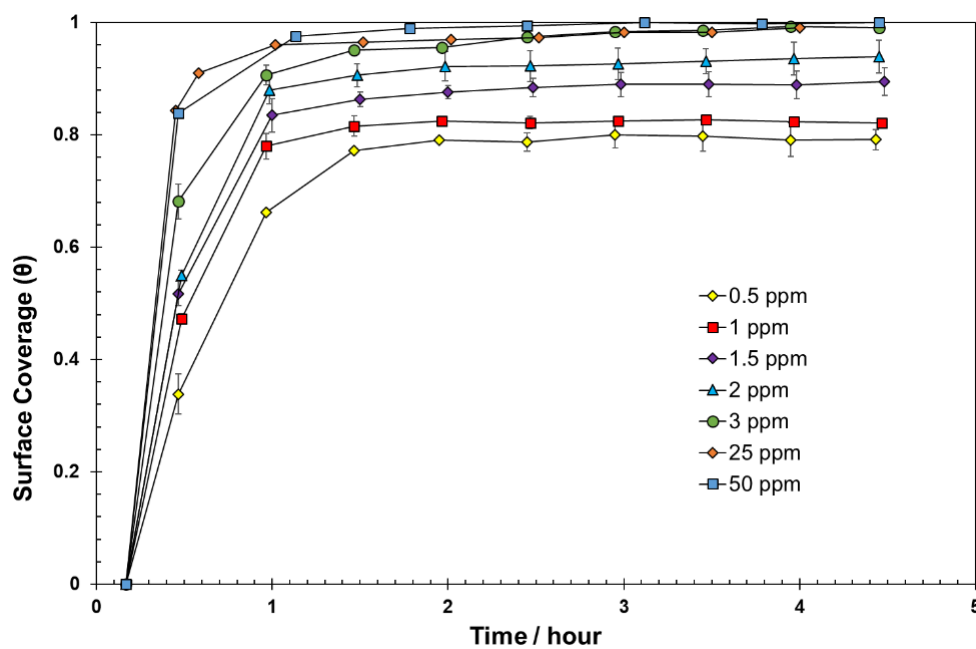


Figure 11: Coverage fraction vs. time in 5 wt.% NaCl (pH = 4.5) with different TPE concentrations at 25°C.

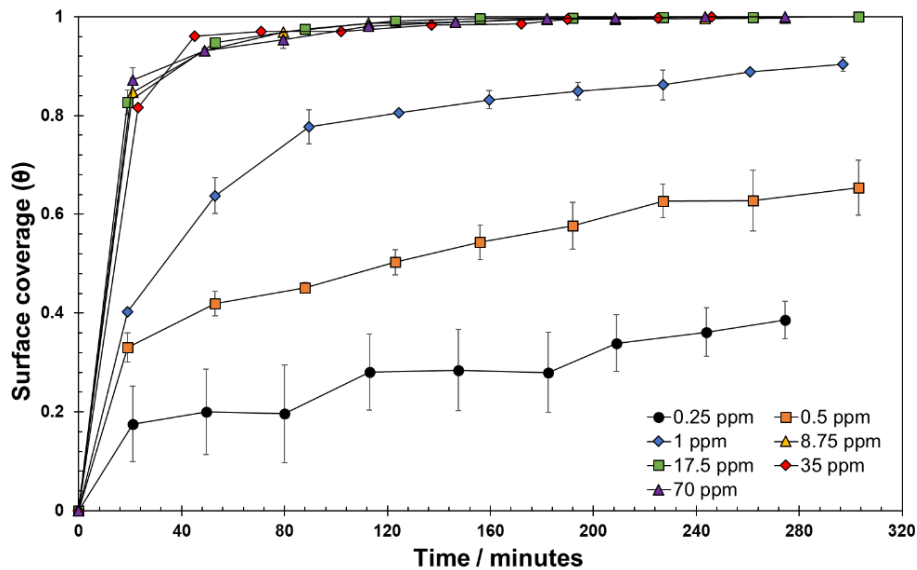


Figure 12: Coverage fraction vs. time in 5 wt.% NaCl (pH = 4.5) with different TTHP concentrations at 25°C.

Table 3
The equilibrium coverage fractions in different TPE concentrations

Conc. (ppm _w)	Conc. (μM)	θ_{eq}
0	0	0
0.5	1.45	0.79
1	2.89	0.82
1.5	4.34	0.90
2	5.78	0.94
3	8.67	1
25	72.25	1
50	144.5	1

Table 4
The equilibrium coverage fractions in different TTHP concentrations

Conc. (ppm _w)	Conc. (μM)	θ_{eq}
0	0	0
0.25	0.6925	0.37
0.5	1.385	0.68
1	2.77	0.83
8.75	24.2	1
17.5	48.5	1
35	97	1
70	194	1

Kinetic Parameters of Adsorption

The Langmuir isotherm was employed in this work to describe the adsorption of inhibitor molecules on the metal surface¹⁴⁻¹⁶. The governing equation of Langmuir adsorption model is given by Equation (2):

$$\frac{d\theta}{dt} = k_A C_{inh}(1 - \theta) - k_D \theta \quad (2)$$

where θ is the surface coverage, t is the time, k_A and k_D are the adsorption and desorption constants of the Cl, respectively, and C_{inh} is the bulk concentration of the Cl.

Equation (2) is a linear ordinary differential equation, which can be solved with the initial condition: $\theta = 0$ at $t = 0$. Equation (3) then gives solution of coverage as a function of time at given concentration of Cl:

$$\theta(t) = \left(\frac{K_{AD} C_{inh}}{1 + K_{AD} C_{inh}} \right) \left(1 - e^{-(k_A C_{inh} + k_D)t} \right) \quad (3)$$

where K_{AD} is the equilibrium constant of adsorption/desorption, which is equal to the ratio of the adsorption and desorption constants.

(1). Steady State Approach

When time approaches infinity, the surface coverage becomes the equilibrium coverage (θ_{eq}), as shown in Equation (4):

$$\theta_{eq} = \frac{C_{inh} K_{AD}}{1 + C_{inh} K_{AD}} \quad (4)$$

Equation (4) can be rearranged into Equation (5):

$$C_{inh} K_{AD} = \left(\frac{\theta_{eq}}{1 - \theta_{eq}} \right) \quad (5)$$

This suggests a linear relationship between concentration and $\theta_{eq}/(1 - \theta_{eq})$. As a result, the equilibrium constant can be determined by plotting the linear relationship of various concentrations and $\theta_{eq}/(1 - \theta_{eq})$ for TPE and TTHP, as shown in Figure 13 and Figure 14, respectively. For model compound TPE, the equilibrium constant (K_{AD}) was then determined as $1.99 \text{ L}\cdot\mu\text{mol}^{-1}$, which was the slope of the fitted line. Similarly, the equilibrium constant for TTHP was determined as $1.18 \text{ L}\cdot\mu\text{mol}^{-1}$.

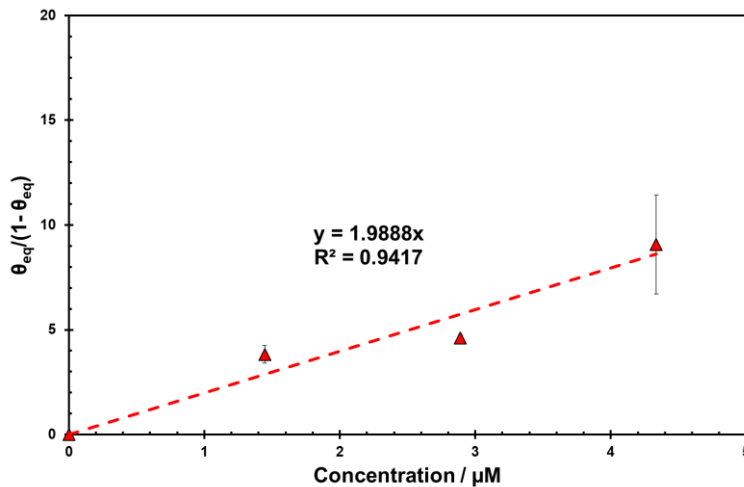


Figure 13: The fitting plot for the relationship of $C_{inh}K_{AD} = \frac{\theta_{eq}}{1-\theta_{eq}}$ for TPE.

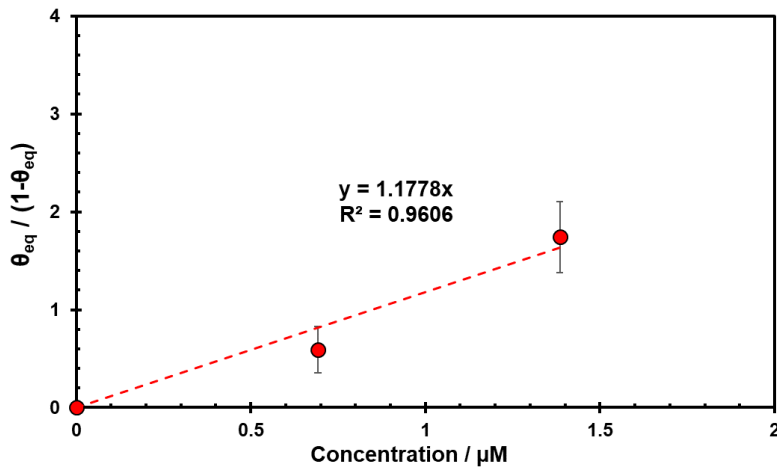


Figure 14: The fitting plot for the relationship of $C_{inh}K_{AD} = \frac{\theta_{eq}}{1-\theta_{eq}}$ for TTBP

(2). Transient Approach

Alternatively, the kinetic parameters of adsorption can be determined using the transient approach. In transient condition, the surface coverage fraction on the metal surface keeps changing with time, which can be described by Equation (3). A non-linear regression method was adopted to determine adsorption (k_A) and desorption (k_D) constants in Equation (3). The fitting results for TPE and TTBP are shown in Figure 15 and Figure 16. For TPE, the k_A and k_D are $204.1 \text{ L}\cdot\text{mol}^{-1}\cdot\text{s}^{-1}$ and $8.6 \times 10^{-5} \text{ s}^{-1}$, respectively. Thus, K_{AD} can be calculated from (k_A / k_D) , as $2.37 \text{ L}\cdot\mu\text{mol}^{-1}$, which is close to K_{AD} from the steady state approach. For TTBP, the k_A and k_D are $108.3 \text{ L}\cdot\text{mol}^{-1}\cdot\text{s}^{-1}$ and $9.07 \times 10^{-5} \text{ s}^{-1}$, respectively. K_{AD} can be calculated as $1.19 \text{ L}\cdot\mu\text{mol}^{-1}$ which is also very close to the value obtained with the steady state approach.

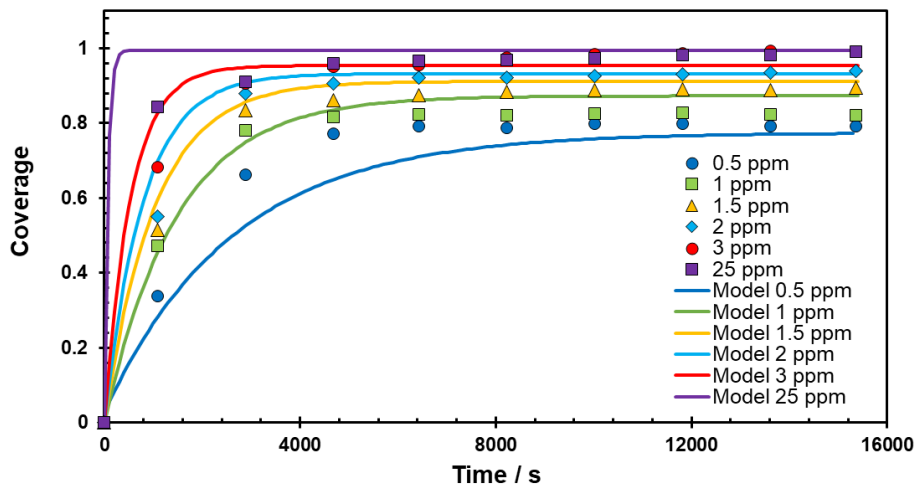


Figure 15: Plot for determination of k_A and k_D by non-linear regression method for TPE.

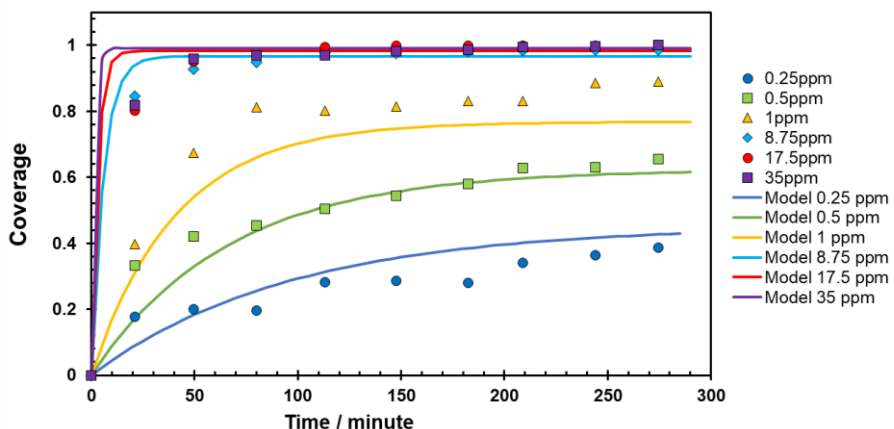


Figure 16: Plot for determination of k_A and k_D by non-linear regression method for TTBP.

CONCLUSIONS

This work presents the development and application of a methodology for CI characterization and inhibition evaluation to two model compounds: tetradecyl phosphate ester (TPE) and tetradecyl tetrahydropyrimidinium (TTBP). Corrosion rate (CR) over various CI concentrations can provide the surface saturation concentration. Moreover, they can be converted to surface coverage fraction, from which adsorption kinetics parameters of CIs can be extracted by fitting experimental results. The CIs performance can be assessed by inhibition efficiency (calculated from CR). Surface saturation concentration could serve as a practical dosing guidance. These results are crucial and practical in oil and gas industry application. The adsorption kinetic parameters can be employed in the establishment of an inhibition prediction model.

Potentiodynamic polarization curves show that the presence of TPE or TTHP retards both anodic and cathodic reactions, while it has no effect on the limiting current density. This behavior indicates that the inhibition model proposed by Dominguez Olivo^{8,9} seems largely applicable for TPE and TTHP, at least within the narrow window of tested experimental conditions (5 wt.% NaCl, pH = 4.5, 25°C). Future will focus on the domain of validity of the inhibition model for these model compounds.

The values of the main parameters determined in present work are as follows, for an aqueous environment of 5 wt.% NaCl (pH = 4.5) at 25°C:

- The surface saturation concentrations of TPE and TTHP were determined: 2-3 ppm_w for TPE and 1-8.75 ppm_w for TTHP.
- The adsorption, desorption, and equilibrium constants of TPE are $k_A = 204.1 \text{ L}\cdot\text{mol}^{-1}\cdot\text{s}^{-1}$, $k_D = 8.6 \times 10^{-5} \text{ s}^{-1}$, and $K_{AD} = 1.99 \text{ L}\cdot\mu\text{mol}^{-1}$, respectively.
- The adsorption, desorption, and equilibrium constants of TTHP are $k_A = 108.3 \text{ L}\cdot\text{mol}^{-1}\cdot\text{s}^{-1}$, $k_D = 9.07 \times 10^{-5} \text{ s}^{-1}$, and $K_{AD} = 1.18 \text{ L}\cdot\mu\text{mol}^{-1}$, respectively.

These values are essential for the next step of the study, which is the validation of the inhibition model initially proposed by Dominguez Olivo^{8,9}.

ACKNOWLEDGEMENTS

This project has been supported by TOTAL transversal R&D project (MANA Project). The authors would like to thank TOTAL for their financial support and valuable discussions.

REFERENCES

1. S. Papavinasam, "Evaluation and Selection of Corrosion Inhibitors," in *Uhlig's Corrosion Handbook: Third Edition*. (Hoboken, NJ, USA: John Wiley & Sons, Inc., 2011), pp. 1121–1127.
2. A. Edwards, C. Osborne, S. Webster, D. Klenerman, M. Joseph, P. Ostovar, and M. Doyle, "Mechanistic studies of the corrosion inhibitor oleic imidazoline," *Corrosion Science* 36, 2 (Feb. 1994): pp. 315–325.
3. E. McCafferty, *Introduction to Corrosion Science*. (New York, NY: Springer New York, 2010).
4. V. S. Sastri, *Green Corrosion Inhibitors*. (Hoboken, NJ, USA: John Wiley & Sons, Inc., 2011).
5. Y. J. Tan, S. Bailey, and B. Kinsella, "An investigation of the formation and destruction of corrosion inhibitor films using electrochemical impedance spectroscopy (EIS)," *Corrosion Science* 38, 9 (Sep. 1996): pp. 1545–1561.
6. M. Finšgar and J. Jackson, "Application of corrosion inhibitors for steels in acidic media for the oil and gas industry: A review," *Corrosion Science* 86 (Sep. 2014): pp. 17–41.
7. S. Seal, K. Satre, A. Kale, V. Desai, M. Gopal, and P. Jepson, "Effect of multiphase flow on corrosion of C-steel in presence of inhibitor: A surface morphological and chemical study," *Corrosion Science* 42, 9 (Sep. 2000): pp. 1623-1634.
8. J. M. Domínguez Olivo, B. Brown, D. Young, and S. Nesić, "Electrochemical model of CO₂ corrosion in the presence of quaternary ammonium corrosion inhibitor model compounds," CORROSION 2019, paper no. 13392 (Houston,TX: NACE, 2019).
9. J. M. Domínguez Olivo, "Electrochemical Model of Carbon Dioxide Corrosion in the Presence of Organic Corrosion Inhibitors," Ph.D. Dissertation, Ohio University (2020).
10. Y. He, S. Ren, Z. Belarbi, X. Wang, D. Young, and M. Singer, "Micellization and Inhibition Efficiency," CORROSION 2021, paper no. 16872 (Houston,TX: NACE, 2021). (in press)
11. Z. Belarbi, F. Farelas, M. Singer, and S. Nešić, "Role of amines in the mitigation of CO₂ Top of the Line Corrosion," *Corrosion* 72, 10 (2016): pp. 1300-1310.
12. R.P.M.W. Jacobs, R.O.H. Grant, J. Kwant, J.M. Marquenie, E. Mentzer, "The composition of produced water from Shell operated oil and gas production in the North Sea." J.P. Ray, F.R. Engelhardt (Eds.), *Produced Water: Technological/Environmental Issues and Solutions*, Plenum Publishing Corp., New York (1992), pp. 13-22
13. T. Murakawa, S. Nagaura, and N. Hackerman, "Coverage of iron surface by organic compounds and anions in acid solutions," *Corrosion Science* 7, 2 (1967): pp. 79-89.
14. Y. Liu and L. Shen, "From Langmuir Kinetics to First- and Second-Order Rate Equations for Adsorption," *Langmuir* 24, 20 (Oct. 2008): pp. 11625–11630.

15. I. Langmuir, "The Adsorption of Gases on Plane Surfaces of Glass, Mica and Platinum..," *Journal of the American Chemical Society* 40, 9 (Sep. 1918): pp. 1361–1403.
16. M. Knag, K. Bilkova, E. Gulbrandsen, P. Carlsen, and J. Sjöblom, "Langmuir–Blodgett films of dococyltriethylammonium bromide and octadecanol on iron. Deposition and corrosion inhibitor performance in CO₂ containing brine," *Corrosion Science* 48, 9 (Sep. 2006): pp. 2592–2613.